Brain (1997), **120,** 1553–1567

Central motor processing in Huntington's disease
A PET study

P. Bartenstein,[1] A. Weindl,[2] S. Spiegel,[1] H. Boecker,[2] R. Wenzel,[1] A. O. Ceballos-Baumann,[2] S. Minoshima[3] and B. Conrad[2]

Departments of [1]Nuclear Medicine and [2]Neurology, Technische Universität München, Germany, and [3]Department of Nuclear Medicine, University of Michigan, Ann Arbor, Michigan, USA

Correspondence to: Peter Bartenstein, MD, Nuklearmedizinische Klinik und Poliklinik der Technischen Universität München, Klinikum rechts der Isar, Ismaninger Str. 22, 81675 München, Germany

Summary
Repeated PET cerebral blood flow measurements using $H_2^{15}O$ were performed in 13 patients with confirmed Huntington's disease and nine age-matched controls. The activation paradigm consisted of an externally triggered finger opposition task (1.5 Hz) with the dominant hand, the control condition being the auditory input. In the patients with Huntington's disease, impaired activity of the striatum and its frontal motor projection areas (rostral supplementary motor area, anterior cingulate and premotor cortex) could be demonstrated along with enhanced activity mainly in parietal areas during movement. The results suggest that the pathology of Huntington's disease causes impairment of the output part of the basal ganglia-thalamo-cortical motor circuit and may induce a compensatory recruitment of additional accessory motor pathways involving the parietal cortex.

Keywords: PET; Huntington's disease; blood flow; activation; motor control

Abbreviations: BA = Brodmann area; FDG = [^{18}F]fluorodeoxyglucose; rCBF = regional cerebral blood flow; rCMRGlc = regional cerebral metabolic rate of glucose

Introduction
Huntington's disease is a progressive neurodegenerative disorder with autosomal dominant inheritance and complete penetrance, but with variable expression. Age of onset is usually between 30 and 50 years, and clinical symptomatology is characterized by the combination of a choreatic movement disorder, intellectual decline and psychopathological changes (Mayeux *et al.*, 1986). Although chorea is the most prominent motor symptom, bradykinesia, rigidity and dystonia are observed as well (Girotti *et al.*, 1984).

The disease-causing mutation, an unstable DNA sequence in the coding region of the Huntington gene on chromosome 4p, has been identified (Huntington's Disease Collaborative Research Group, 1993). This expansion of a $(CAG)_n$ trinucleotide repeat can be detected using the polymerase chain reaction, thus providing a direct gene test. In Huntington's disease patients, the number of repeats ranges from 37 to 121 in comparison with 9 to 36 in the normal population (Martin, 1993). The length of the trinucleotide repeat and age of onset show a positive correlation (Duyao *et al.*, 1993).

The characteristic pathological finding in Huntington's disease is a loss of small to medium size spiny neurons, beginning in the dorsal medial head of the caudate with subsequent progression to the ventrolateral striatum (Vonsattel *et al.*, 1985; Myers *et al.*, 1988). A less pronounced neuronal loss is also found in palaeostriatum, substantia nigra, thalamus, hypothalamus, cerebellum and cortical areas (Lange *et al.*, 1976; Vonsattel *et al.*, 1985; Myers *et al.*, 1991). Corresponding to these changes at the neuronal level, glucose metabolism measured by [^{18}F]fluorodeoxyglucose (FDG)-PET is severely reduced in the caudate and moderately reduced in the lentiform nucleus at very early stages of disease, even before patients become symptomatic (Kuhl *et al.*, 1982; Leenders *et al.*, 1986; Kuwert *et al.*, 1993). Cortical metabolism is not reduced at initial stages of the disease but with progression a pronounced frontal hypometabolism becomes apparent (Grafton *et al.*, 1992; Kuwert *et al.*, 1993).

At the level of the basal ganglia, combined studies of neurotransmitter markers and neuronal density measurements

© *Oxford University Press 1997*

Table 1 *Clinical features of the 13 Huntington's disease patients included in the analysis*

	Group 1 ($n = 7$) Mean (range)	Group 2 ($n = 6$) Mean (range)
Age (years)	45 (27–69)	61 (54–73)
Age of onset (years)	41 (22–66)	55 (42–68)
Duration of disease (years)	4 (3–6)	6 (2–12)
Abnormal Involuntary Movement Scale (score)	1 ($n = 7$)	1 ($n = 2$); 2 ($n = 4$)
Number of CAG repeats	46 (42–50)	45 (42–48)
CAMCOG (score)	78 (67–87)	57 (49 –64)

have shown that pertinent reductions of 'small' size spiny neurons in Huntington's disease are directly correlated with decreases in GABA concentration (Kanazawa *et al.*, 1985). This predominant loss of striatal GABAergic neurons projecting from neostriatum to globus pallidus and substantia nigra directly affects basal ganglia output to the cortex. Hence, the primary aim of this study was to identify changes of motor-associated cortical activation at a stage of disease when no major cortical abnormalities are present. A PET activation study using a sequential motor task was performed for this purpose.

Methods

Subjects

A total of 15 right-handed patients with inherited Huntington's disease and nine age-matched normal volunteers were studied.

The patients were examined by two experienced neurologists who defined the extent of hyperkinesia using the Abnormal Involuntary Movement Scale according to Lane *et al.* (1985). According to this scale, the hyperkinesia in all cases was mild to moderate (Table 1). Only three of the patients had a very mild, hardly detectable degree of rigidity. Pronounced rigidity present in the Westphal variety of Huntington's disease was not observed. Clinically, bradykinesia was not apparent in these patients, although precise data were not available for all cases to enable us to quantify its presence or absence. In addition, the intellectual impairment was measured using the appropriate section (CAMCOG) of the Cambridge Mental Disorders of the Elderly Examination (CAMDEX) (Roth *et al.*, 1986).

The diagnosis of Huntington's disease was confirmed by measurements of CAG repeat length (Huntington's Disease Collaborative Research Group, 1993). All patients included in the study had a CAG repeat length above 40. The mean disease duration was 4 years (range, 2–12 years). All patients underwent CT scans of the brain to exclude any structural lesions of the basal ganglia and other conditions that could have potentially affected the stereotactic normalization of the PET scans (*see* below). Caudate atrophy in all patients did not exceed a moderate degree. No patient had a history of cerebrovascular disease, hypertension or diabetes.

Two patients were excluded from the subsequent analysis because they exhibited uncontrolled involuntary choreatic movements during the PET study, which interfered with the motor task. During the scans all other patients showed either no choreatic movements or only very mild ones, which were barely visible in most cases and did not interfere with the sequential motor task.

In order to generate a homogenous group of Huntington's disease patients comparable to the control population, the remaining 13 patients were separated into two groups according to their performance in the motor task during the PET study. A total of seven patients were able to perform the motor task with a 100% response to the given external trigger signal and with a failure rate of $<25\%$ (*see* below). This group of patients (Group 1) was used for the statistical comparison with the normal database. It consisted of four females and three males; age range 27–69 (mean 45 years).

The remaining six patients had a higher failure rate and/or did not show a 100% response to the external trigger (Group 2). Their motor performance did not match that of the control group; therefore, these patients were only included in the correlation analysis (*see* below). In this group all patients except one were female, and their age ranged from 54 to 73 (mean 61 years). The clinical characteristics of all patients are summarized in Table 1. The groups did not differ as far as duration of disease and CAG repeat length were concerned. They were, however, different according to measures of intellectual impairment ($P < 0.001$) and age of onset ($P < 0.01$).

For statistical comparisons, nine age-matched, right-handed control subjects were studied (four females, five males; age range 34–71; mean 54 years). None had a history of neurological or any severe internal disease. Handedness in patients and controls was determined by the Edinburgh handedness inventory (Oldfield, 1971).

In accordance with the declaration of Helsinki, all control subjects and patients gave their informed written consent to participate in the study after the experimental procedure and radiation effects had been explained. The experiment had the approval of the Ethics Committee of the Faculty of Medicine of the Technical University, Munich and the radiation protection authorities.

Paradigm design

The paradigm used was a modification of a motor task described in previous PET studies (Colebatch *et al.*, 1991; Weiller *et al.*, 1992).

Each subject was scanned six times in the same session. Scans were performed under two conditions: (i) at rest; (ii) during sequential, finger-to-thumb opposition of the right, dominant hand. The rate of opposition was driven by a metronome at two oppositions every 3 s. This rate was chosen to allow as many patients as possible to perform the

task accurately and to have a sufficiently high amount of motor actions during the scanning period. To control for activation due to auditory input, the metronome sounded during all six scans. Brief training was given to each subject prior to the scanning. To avoid systemic effects due to habituation, an alternating sequence of the two conditions was used, varying the starting condition in a random order. Scans were performed with the subjects' eyes open in dimmed, ambient light. To avoid visual control of the movements, the hand was placed outside the visual field and the subjects were instructed not to control their finger movements visually.

Measurement of motor performance

To measure motor performance in the finger opposition task, we used a force transducer which was fixed to the thumb of the subjects. With a commercially available tape recording machine, we recorded the pressure of each fingertip on one channel and the sound of the metronome on a second channel. From these recordings, error score and response time for each subject were calculated. During the scans, the patients were monitored by two video cameras to exclude involuntary movements of all limbs and to control the exact sequence of finger opposition.

A motor action was considered as being a failure when a finger other than the next in the sequence was used. If the next finger or the index finger were used after a failure, this was not considered a mistake. When they had problems in continuing, patients and subjects were instructed to start again with the index finger.

PET scanning and image reconstruction

PET measurements were performed using a Siemens 951 R/31 PET scanner (CTI, Knoxville, Tenn., USA) in two-dimensional mode with a total axial field of view of 10.5 cm and no inter-plane dead space under standard resting conditions (eyes open in dimmed ambient light). Attenuation was corrected using a transmission scan with an external $^{68}Ge/^{68}Ga$ ring source obtained prior to the tracer injection.

A semibolus injection of 40 mCi $H_2^{15}O$ was administered intravenously over 35 s using an infusion pump. A dynamic acquisition protocol was performed starting with the infusion: it consisted of a sequence of eight short-duration frames: one 15 s frame followed by seven 10 s frames, covering a total scan time of 85 s. The motor task started with the beginning of the scan.

Following corrections for randoms, dead time and scatter, images were reconstructed by filtered back-projection with a Hanning filter (cut-off frequency 0.4 cycles/projection element), resulting in 31 slices with a 128×128 pixel matrix (pixel size 2.0 mm) and interplane separation of 3.375 mm. Since time–activity curves of the whole brain showed initial tracer appearance during scan 4 and its maximum between scans 4 and 8 in all subjects, frames 4–8 were added to a single frame consisting of 50s for further analysis.

Statistical analysis

Determination of areas showing regional cerebral blood flow increase during activation within each group

Tracer counts were proportionally normalized to the global cerebral activity, which was arbitrarily set to 1000, in order to perform analysis on relative tissue regional cerebral blood flow (rCBF) activity (Fox and Raichle, 1984). An automated program (Statistic Parametric Mapping Software from the University of Michigan; SPMS-Mich.) to coregister, reslice and transform the image arrays into the stereotactic space of Talairach and Tournoux (1988), as described previously (Minoshima *et al.*, 1993, 1994), was used. To eliminate individual differences in gyral anatomy, these images were further smoothed with a three-dimensional Gaussian filter to give an effective resolution of ~18 mm (full width half maximum). Repeated control and activation images were averaged for each within a subject. Differences between control and activation images were then averaged across subjects and were expressed as voxel-by-voxel *t* statistic values using a pooled variance estimated from the whole brain grey matter (Worsley *et al.*, 1992). Since the resulting *t* statistic map by the method described above is known to be a good approximation for a standard Gaussian distribution (Worsley *et al.*, 1992), we describe those values as *Z*-scores. In order to determine a threshold for significant activation on the resulting *Z*-map, we calculated the image smoothness (Friston *et al.*, 1991) and estimated a statistical threshold at a one-tail (positive) probability of $P = 0.05$ using a statistical model which adjusts multiple comparisons and the inherent correlation of neighbouring voxels (Montreal threshold) (Worsley *et al.*, 1992).

These comparisons were performed independently for the nine normal volunteers and the seven patients of Group 1.

Comparison of rCBF increases during activation

In addition to these comparisons within each group (normal subjects and the patients of Group 1), we sought to identify areas in which the task in the patients evoked more or less activation in the patients than in the control subjects. This was done by comparing the changes in rCBF between the rest and the activation condition between groups in order to identify voxels at which these changes were significantly different. To compare differences in activation between the groups the adjusted error variance was estimated for each group and its mean was used to compute the *t* statistics. A one-tailed *t* test was used and a significance level of 0.01 without correction for multiple comparisons was allowed (Kew *et al.*, 1993). To exclude the detection of subtle differences in areas where no relevant or only inconsistent

Table 2 *Areas with significantly decreased FDG uptake under resting conditions in patients of both groups*

Area	HD patients (Group 1) ($n = 7$)					HD patients (Group 2) ($n = 6$)				
	Talairach coordinates			*Z*-score (significance level)	% difference in normalized rCMRGlc	Talairach coordinates			*Z*-score (significance level)	% difference in normalized rCMRGlc
	x	*y*	*z*			*x*	*y*	*z*		
Right caudate nucleus	–10	10	14	6.3 ($P < 0.0001$)	49	–10	12	9	6.3 ($P < 0.0001$)	53
Left caudate nucleus	6	12	11	5.3 ($P < 0.0001$)	41	6	12	9	6.3 ($P < 0.0001$)	52
Right putamen	–21	3	2	5.1 ($P < 0.0001$)	40					
Left putamen	21	1	0	4.9 ($P < 0.0001$)	36					
Right anterior cingulate (BA 24)						–3	14	20	4.5 ($P < 0.0001$)	37

Brain areas showing significant decreases in rCMRGlc (above the Montreal threshold) under resting conditions in the patients in Groups 1 and 2 compared with seven age-matched controls. The Talairach coordinates, the *Z*-score and the relative decrease of rCMRGlc of the voxel in each area showing the maximum significant difference are listed. HD = Huntington's disease.

activation had occurred, this analysis was restricted to voxels where rCBF increases during activation in either the patients group or the normal subjects achieved a *Z*-score above 1.64 ($P = 0.05$, one tail) (Wenzel *et al.*, 1996). To estimate the change in normalized rCBF, the voxels showing maximally different motor task activation were used.

Correlation analysis

To assess the effect of the failure rate on the areas of motor planning and motor execution, Pearson's linear correlation was performed on a pixel-by-pixel basis. The correlation coefficient was used after Fischer's transformation to calculate the *Z*-values. This analysis was again restricted to voxels where activation in either the patients group or the normal subjects achieved a *Z*-score above 1.64. This correlation analysis was done using the data of all 13 patients, deliberately including patients with a wide range of error scores during task performance. A correlation analysis using the motor actions performed during the scanning period as the external variable was performed as well in these patients.

FDG–PET of patients

To confirm the presence of striatal metabolic reduction in all patients and to determine other areas of potentially impaired glucose consumption under resting conditions, an additional measurement of cerebral metabolic rate for glucose (rCMRGlc) was performed using the same scanner, reconstruction and correction parameters as described above. All FDG scans were performed within an interval of 2 months of the activation study. PET images were obtained 30 min after the intravenous administration of 10 mCi FDG. They comprised a sequence of three frames of 10 min duration which were later added to a single frame. Unfortunately, there were no quantitative data available for some of the patients, and therefore a semiquantitative comparison had to be performed.

To confirm the striatal metabolic reduction in each patient, an automatic realignment of the image set to the bicommissural line (AC–PC line), as described previously (Minoshima *et al.*, 1993), was performed prior to anatomical standardization in the stereotactic system using linear and non-linear warping techniques (Talairach and Tournoux, 1988; Minoshima *et al.*, 1994). Striatal metabolic activity was analysed semiquantitatively after normalization to the global mean and was compared with an image database consisting of seven age-matched normal controls scanned under similar conditions (mean age 47, range 31–71 years). To quantify the metabolic deficits, the normalized striatal activity of each patient was compared with the normal database on a pixel-by-pixel basis by means of a *Z*-score. A positive *Z*-score here represents a reduced rCMRGlc in the patient relative to the control mean. The derived data were displayed as *Z*-score images using transversal images (Minoshima *et al.*, 1995). From these *Z*-score images, the mean *Z*-scores for the striatum of both sides were derived using a predefined set of regions of interest covering the respective areas.

In addition, an across-subject comparison was performed between Group 1 and the seven age-matched controls. The same comparison was done with the six patients of Group 2 and the seven controls. For these comparisons, tracer counts were proportionally normalized to the global cerebral activity in a way equivalent to that described above (Fox and Raichle, 1984) using the same automated program (SPMS-Mich.) to coregister, reslice and transform the image arrays into the stereotactic space of Talairach and Tournoux (1988). To eliminate individual differences in gyral anatomy, these images were further smoothed with a three-dimensional Gaussian filter to give an effective resolution of ~18 mm (full width half maximum). Differences between patient and

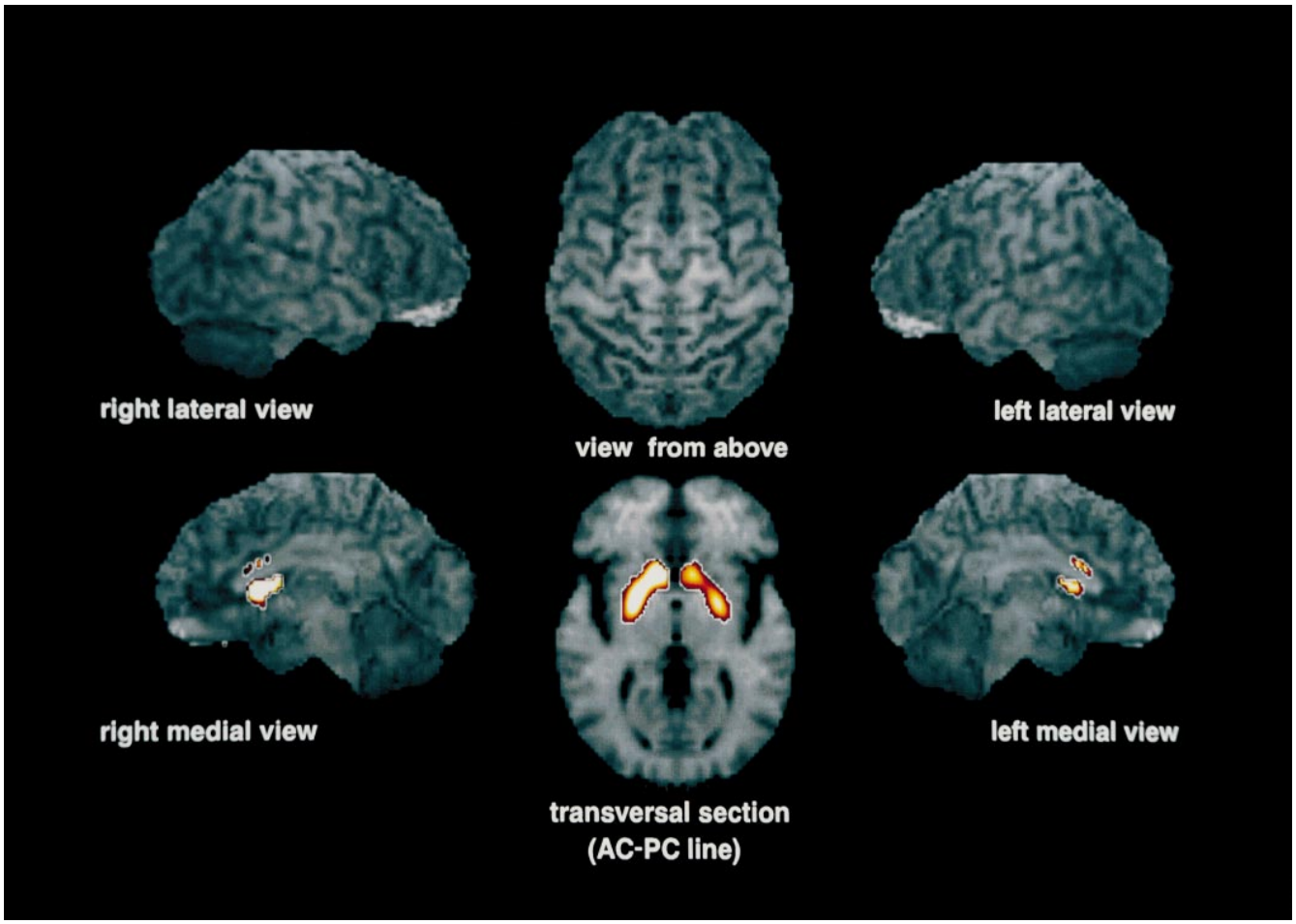

Fig. 1 Comparison of the rCMRGlc under resting conditions between the patients of Group 1 ($n = 7$) and seven age-matched controls. For illustrative purposes all voxels are displayed where the decrease of rCMRGlc in the patients reached a significance level of 0.001, not corrected for multiple comparisons. Transversal images are oriented with the left side of the brain on the right side of the image.

control images were expressed as *Z*-scores. In order to determine a threshold for significant differences on the resulting *Z*-map, the image smoothness was calculated (Friston *et al.*, 1991) and a statistical threshold at one-tail (positive) probability of $P = 0.05$ was estimated using a statistical model which adjusts multiple comparisons and inherent correlation of neighbouring voxels (Montreal threshold) (Worsley *et al.*, 1992). To quantify the decrease in rCMRGlc the relative difference of normalized rCMRGlc between patients and controls in the voxel exhibiting the highest *Z*-score was determined.

Results

Measurement of motor performance

When performing the motor task, the normal volunteers had a mean failure rate of 0.2% and all normal volunteers had $<1\%$ incorrectly performed actions.

For the patients in Group 1, the failure rate was $<25\%$ in all cases. The mean failure rate in this patient group was 8%, ranging from 2 to 22%. The other six patients (Group 2) performed very heterogeneously. They all performed $>80\%$ of the motor actions. The mean failure rate was 41% for these patients (range 19–80%).

Determination of rCMRGlc in the resting state

Striatal glucose consumption was substantially reduced in all patients scanned. The *Z*-score images derived for each individual revealed a mean *Z*-score below the normal database of 3.4 (range 2.5–5.8) for patients of Group 1 and a mean *Z*-score of 3.9 (range 2.9–5.7) for Group 2. Striatal glucose consumption was not statistically different between the two groups.

The across-subject comparison between Group 1 and seven age-matched controls showed significant decreases in rCMRGlc ($P < 0.05$) in the striatum of both sides. Table 2 summarizes the areas where the increases reached a *Z*-score above the estimated threshold of 4.31 for $P = 0.05$,

considering multiple comparisons and the inherent correlation of neighbouring voxels.

In this comparison the only other area showing a decreased rCMRGlc above the 0.001 significance threshold (not corrected for multiple comparisons) was located in the anterior cingulate [Brodmann area (BA) 24]. The Talairach coordinates of the voxel reaching maximum statistical significance were $x = 1$; $y = 19$; $z = 18$; the average decrease of normalized rCMRGlc in this voxel was 19% (Fig. 1). Differences in rCMRGlc in motor-associated areas of the frontal cortex (central, premotor, prefrontal cortex and supplementary motor area with adjacent parts of the cingulate) did not reach significance above the threshold of 0.01 (not corrected for multiple comparisons).

The comparison between Group 2 and the seven controls revealed significant differences in the striatum of both sides and in the anterior cingulate. There were no differences in rCMRGlc in other motor associated areas of the frontal cortex above the threshold of 0.01 (not corrected for multiple comparisons in this group also). The right part of Table 2 gives summaries of the areas where the increases in this comparison reached a *Z*-score above the estimated threshold of 4.49 for $P = 0.05$, considering multiple comparisons and the inherent correlation of neighbouring voxels.

Determination of areas showing rCBF increase during activation within each group

In the normal controls, the stereotyped motor task induced significant increases in rCBF ($P < 0.05$ corrected for multiple comparisons) in the contralateral (left) primary sensorimotor cortex, the dorsal and rostral supplementary motor area with adjacent parts of the cingulate gyrus, the bilateral premotor cortices (BA 6), the inferior parietal cortices (BA 40), the ipsilateral cerebellum and the contralateral striatum (Fig. 2A)

When patients performed the finger opposition task, they activated the left sensorimotor cortex, the part of the supplementary motor area dorsal to the anterior commissure (dorsal supplementary motor area), the inferior parietal cortices and the ipsilateral cerebellum to the same extent. In contrast to controls, there was no activation reaching the given significance level in the left striatum, the lateral premotor cortices of both sides and the rostral part of the supplementary motor area with the adjacent part of the anterior cingulate (Fig. 2B; Table 3). For further analysis and description, the supplementary motor area was separated into a dorsal (dorsal supplementary motor area) and rostral part (pre-supplementary motor area); the border between the two parts was defined by the anterior commissure (Stephan *et al.*, 1995).

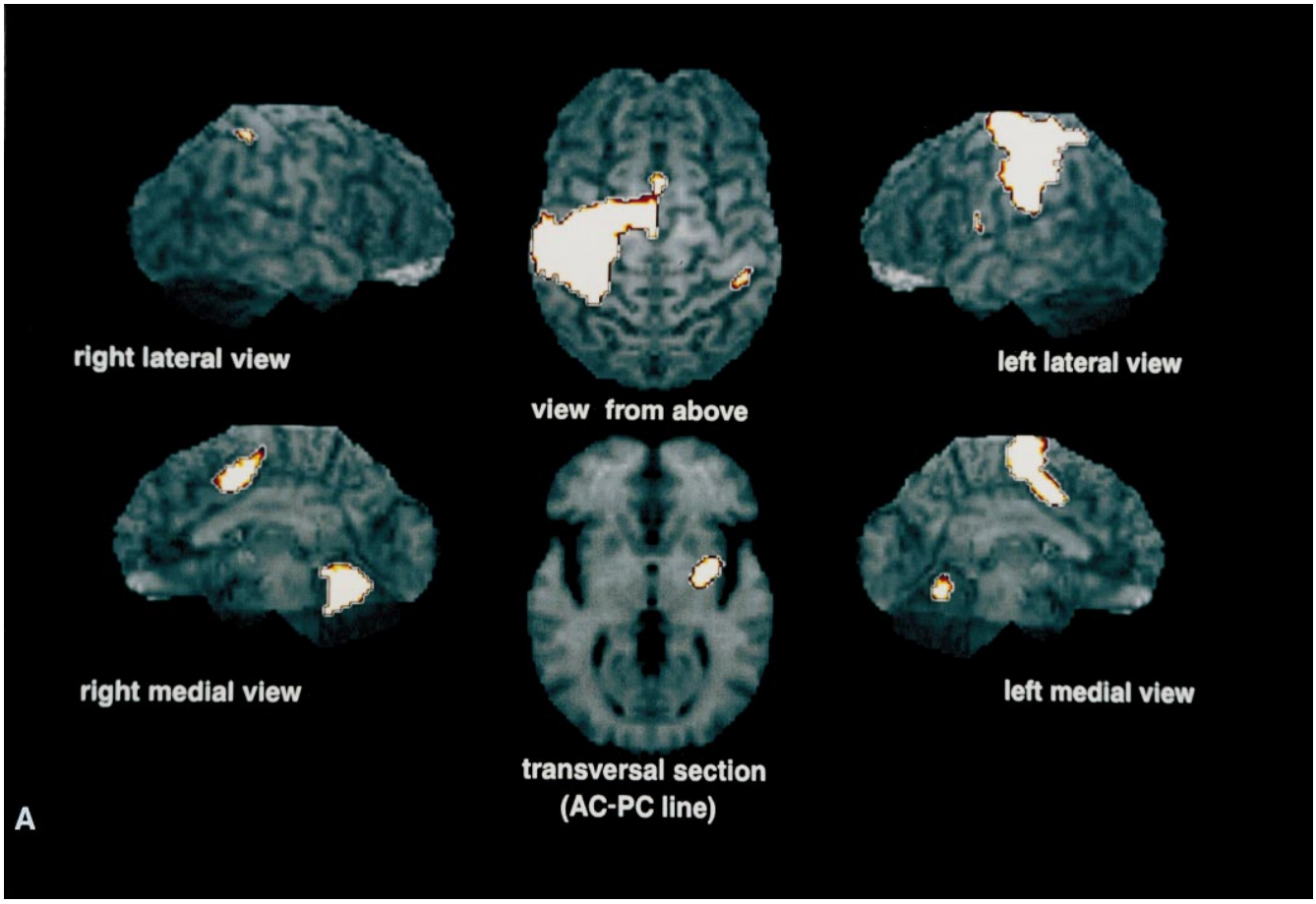

Table 3 summarizes the areas where the increases reached a *Z*-score above the estimated threshold of (4.62 in controls, 4.36 in patients) for $P = 0.05$, considering multiple comparisons and the inherent correlation of neighbouring voxels.

Determination of differences in activation between controls and patients

In the Huntington's disease patients of Group 1, testing activation differences confirmed impaired activation in the left striatum of both premotor cortices and the rostral part of the supplementary motor area along with the adjacent anterior cingulate and the right sensorimotor cortex (Fig. 3A; Table 4A). The significance level reached in the left striatum, rostral supplementary motor area/anterior cingulate, left premotor cortex and right sensorimotor cortex was $P < 0.01$. For the right premotor cortex it was $P < 0.001$. The cerebellum was not included in the SPMS-Mich. analysis because it was not in the field of view in all studies.

In some areas there was significantly higher activation in the patients of Group 1 compared with the controls. These were mainly the right parietal cortex (BA 7 extending to BA 40), reaching a maximum significance level of $P < 0.001$, the left parietal cortex (BA 40) and the posterior cingulate (BA 31), at a significance level of $P < 0.01$, along with a small area of the most inferior part of the right premotor cortex BA 6 (Fig. 3B; Table 4B).

Correlation analysis

Pearson's linear correlation on a pixelwise basis including all 13 patients with Huntington's disease from both groups revealed a significant negative correlation between the failure rate and neuronal activity, inducing relative rCBF changes in the supplementary motor area predominantly rostral to the intercommissural line and adjacent parts of the cingulate (BA 6/24/32), reaching a significance level above $P < 0.01$. The same appeared to be true for a smaller area of the left parietal cortex at the border of BA 2 and BA 40. This indicates that there was a decrease of activation in these areas with a decrease in task accuracy, reflecting impaired higher order motor control (Fig. 4). Table 5 summarizes the areas showing negative correlation with the failure rate, their

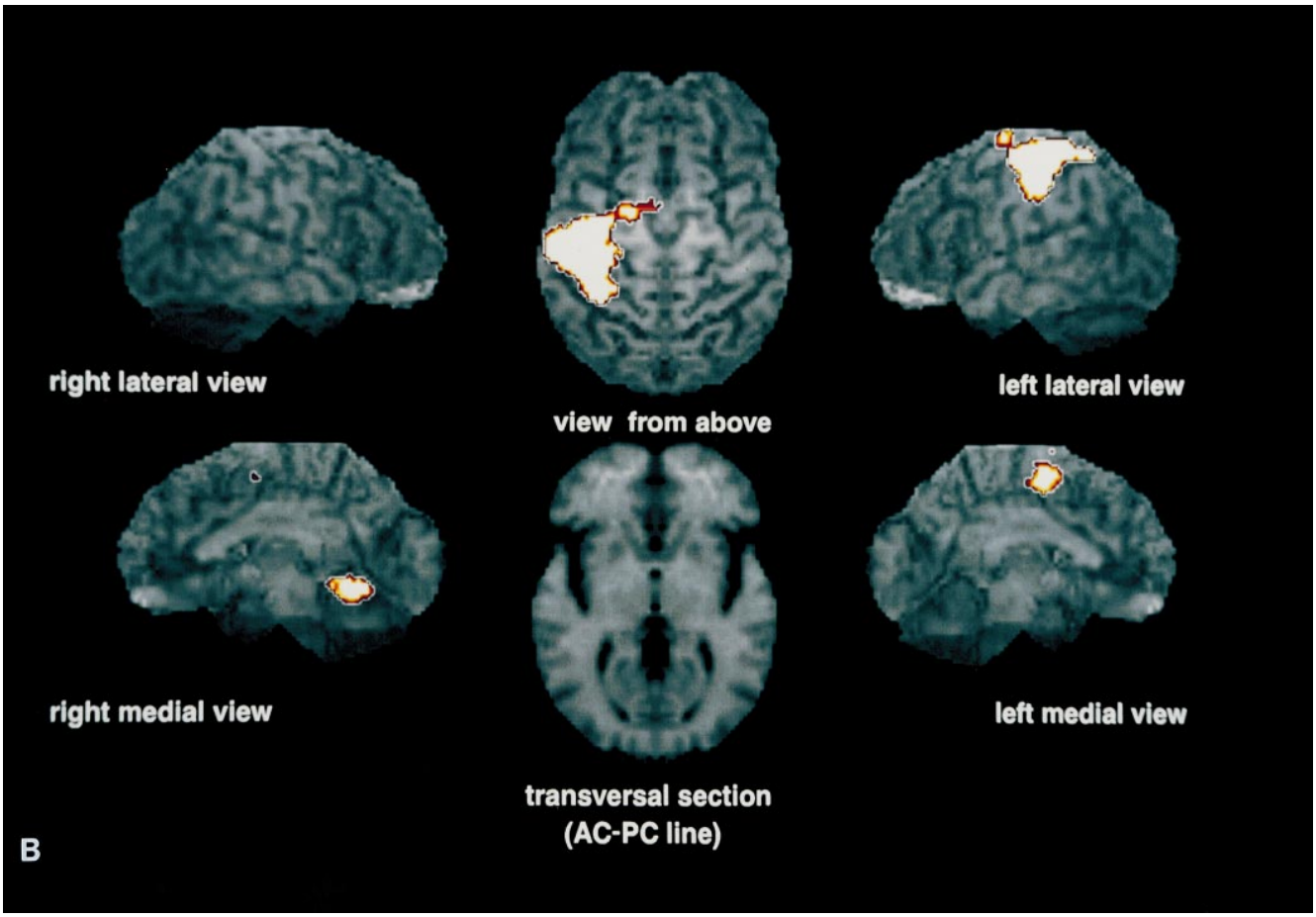

Fig. 2 Comparison of the activation conditions versus rest. (**A**) Control group ($n = 9$). (**B**) Huntington's disease patients (Group 1) ($n = 7$). Increases of rCBF during the automated motor task. All significant voxels above the adjusted statistical threshold (controls = 4.62; patients = 4.36; $P < 0.05$ corrected for multiple comparisons) are displayed. All voxels displayed white indicate a *Z*-score >5. Shaded areas of the normalized MRI indicate areas not in the field of view in all subjects.

Talairach coordinates, the regression coefficient *r*, their *Z*-scores and their significances.

The correlation analysis using the motor actions as the external variable did not reveal areas with a significant correlation (above $P < 0.05$).

Discussion

Methodological considerations

In the normal volunteers, the automated motor task used in the present study showed a significant rCBF increase in contralateral (left) primary sensorimotor cortex, supplementary motor area with adjacent parts of the cingulate, bilateral premotor cortices (BA 6), inferior parietal cortices (B 40), ipsilateral cerebellum and contralateral striatum. This pattern was very similar to the pattern described in previous studies using an equivalent paradigm (Colebatch *et al.*, 1991; Weiller *et al.*, 1992). By incorporating the same methodological approach as Colebatch *et al*. (1991), the average increase of the maximum significant voxel, the increase in the sensorimotor cortex of the normal volunteers in the present study was 24%. This is consistent with the data from Colebatch *et al*. (1991), who reported 21% flow increase during a finger opposition task, and Fox *et al*. (1985), who reported a 24% increase during fist-making for the sensorimotor cortex. The Talairach coordinates of the maximum increase in the normal volunteers for the sensorimotor cortex determined by the statistical mapping method used in the present study were very similar to the coordinates reported by Colebatch *et al.* (1991) and Weiller *et al.* (1992) for this task. This suggests that there were no methodological differences present which would introduce a systematic bias between the method used in the present study and methods used by these authors and others whose results are discussed below. Indeed we have reanalysed our data using another pixel-based statistical analysis program (SPM 95; Wellcome Department of Cognitive Neurology, London UK) and have reconfirmed all the main results reported here with SPMS-Mich.

Patients who were used to compare the rCBF increases during activation performed the same number of motor actions and had no abnormalities in rCMRGlc in the sensorimotor cortex or other motor-related areas of the frontal lobe under resting conditions compared with the controls. The frontal decrease of rCMRGlc was restricted to the most anterior part of the cingulate, which can be attributed to the limbic part of the basal ganglia–thalamocortical circuits rather than to the motor part (Alexander *et al.*, 1990). Consequently, no major differences between the patients and the controls in the activation of the sensorimotor cortex were detectable

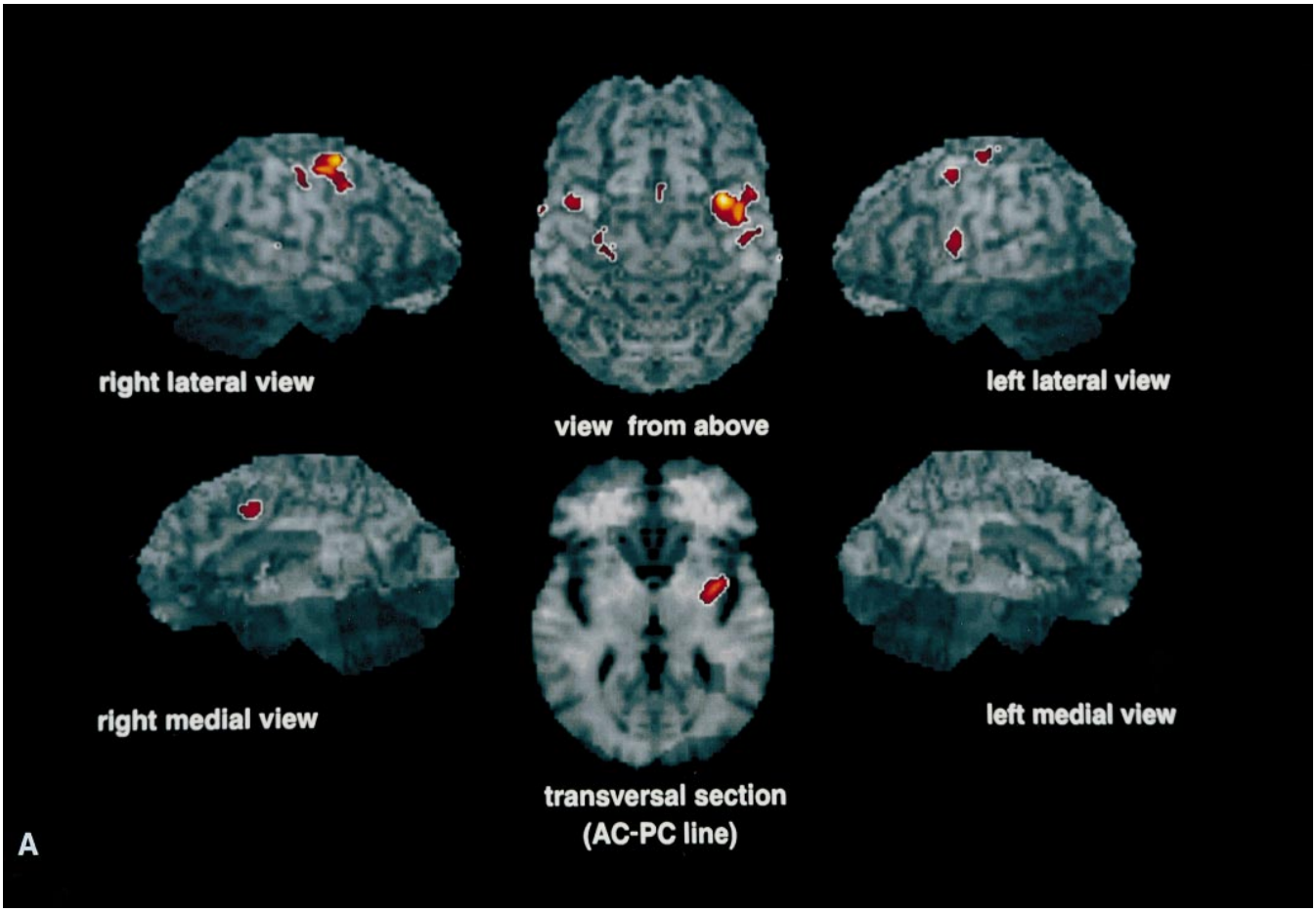

during the task. Similar findings have been reported for other disorders inducing dysfunction of the basal ganglia, for instance for striatocapsular infarction (Weiller *et al.*, 1992). In Parkinson's disease, impaired striatal activation did not result in relevant differences in the activation of the sensorimotor cortex either (Playford *et al.*, 1992). In contrast to this, patients with idiopathic dystonia, as with Huntington's disease, a primarily hyperkinetic extrapyramidal disorder, exhibited in addition to striatal overactivity a bilateral reduced activation of both sensorimotor cortices in a joystick paradigm (Ceballos-Baumann *et al.*, 1995).

Impaired activation in patients with Huntington's disease

As expected, a decrease in glucose metabolism in the resting state and significant impairment in activation were observed in the striatum of all patients with Huntington's disease. This finding demonstrates the bilateral impairment of striatal function specific for this disease present in all patients and the dysfunction of these nuclei during motor activation (Hallet and Ravits, 1986). The impairment of striatal glucose metabolism during the resting condition was not predictive for the ability to perform the automated motor task required in this study.

Areas showing impaired activation in the patients were, besides the putamen, mainly located in the frontal cortex. It was possible to demonstrate that parts of the premotor cortex and of the supplementary motor area with adjacent cingulate areas are not adequately activated in the Huntington's disease patients. The hypoactivity of these areas during the motor action was bilateral.

The activation of the supplementary motor area rostral to the anterior commissure and adjacent areas of the cingulate was closely correlated with the ability of the patients to perform the task accurately. Although some of the patients used for the correlation analysis performed slightly fewer motor actions, it is unlikely that these differences (<20%) are responsible for the hypoactivity of these non-primary motor areas. First, there was no correlation between the motor actions performed and the activation of the supplementary motor area with the adjacent cingulate. Furthermore, Blinkenberg *et al.* (1996) demonstrated in their PET study, using a repetitive motor task with different tapping

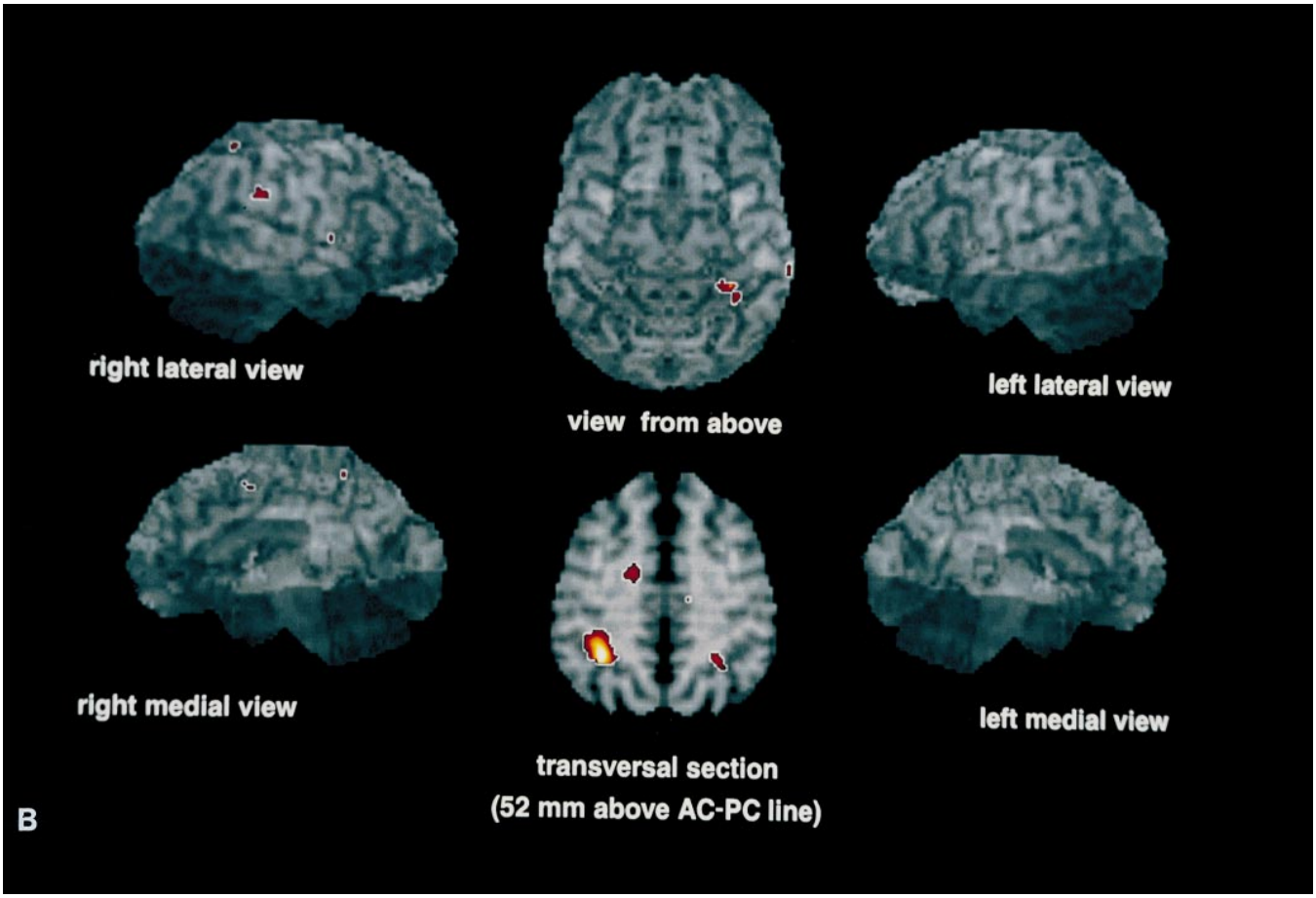

Fig. 3 Comparison of the differences in activation between the control group and the patients of Group 1 ($P < 0.01$ not corrected). (**A**) Voxels that showed significantly greater activation in the control group. (**B**) Voxels that showed significantly greater activation in the patient group.

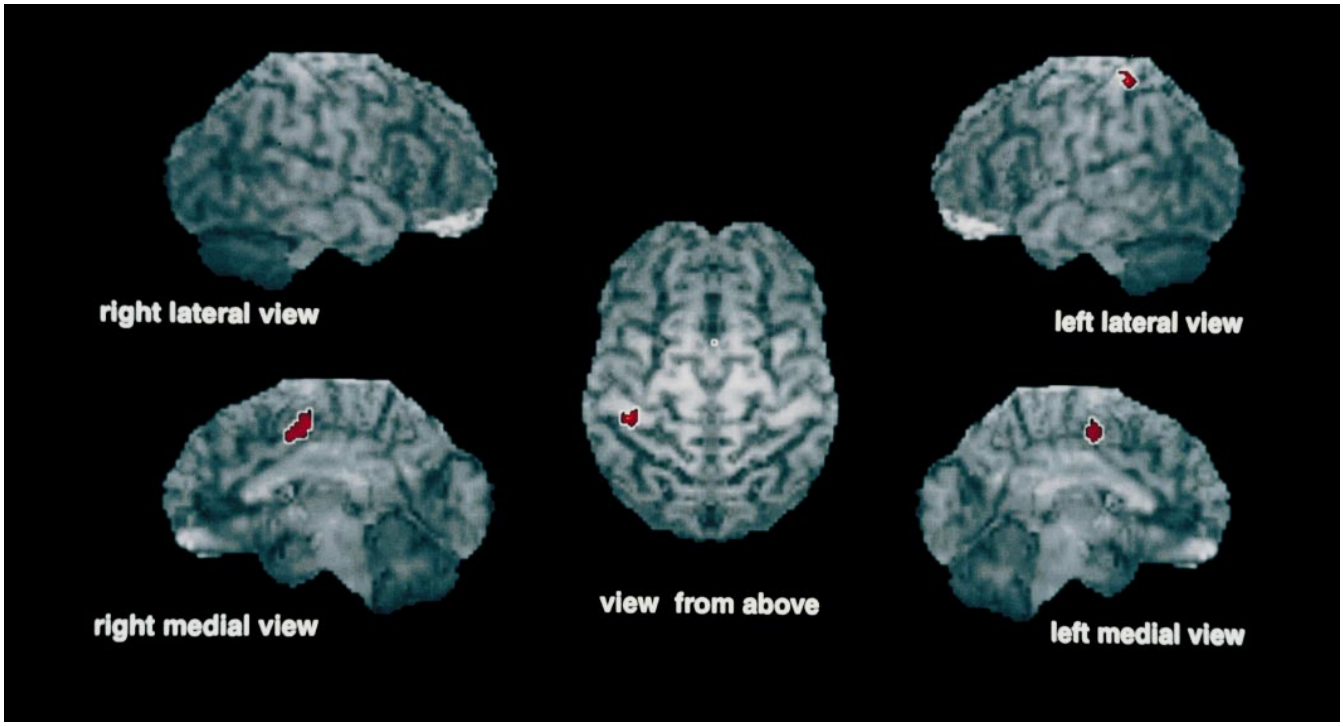

Fig. 4 Correlation analysis showing the voxels with significant correlation to the failure rate ($P < 0.01$ after Fisher's transformation from r to Z). This analysis was based on all 13 patients included in the study. The voxels showing negative correlation with the failure rate are displayed, demonstrating areas where better performance was associated with a higher increase in rCBF.

Table 3 *Areas with significant rCBF increases during the motor task*

Area	Controls ($n = 9$)				HD patients ($n = 7$) (Group 1)			
	Talairach coordinates			*Z*-score	Talairach coordinates			*Z*-score
	x	*y*	*z*		*x*	*y*	*z*	
Left striatum	28	–4	2	6.7				
Left sensorimotor cortex (BA 4)	33	–22	52	14.8	35	–19	50	10.0
SMA rostr./ant. cing. (BA 6/24/32)	–1	8	40	7.5				
SMA dorsal (BA 6)	6	–8	56	7.1	10	–4	52	5.5
Left premotor cortex (BA 6)	51	3	14	5.1				
Left parietal cortex (BA 40)	50	–36	44	8.4				
Right premotor cortex (BA 6)	–24	–4	56	4.8				
Right parietal cortex (BA 40)	–44	–37	50	5.2	–39	–33	38	4.5
Right cerebellum	–17	–51	–18	10.7	–12	–55	–9	5.6

Brain areas showing significant increases in rCBF (above the Montreal threshold) during the motor task. The Talairach coordinates and the *Z*-score of the voxel in each area showing maximum significance are listed. On the left side the areas with significant increases in the control population are listed and on the right side in the patients of Group 1. HD = Huntington's disease; SMA = supplementary motor area.

frequencies, that the activation of non-primary motor areas such as the supplementary motor area is not frequency-dependent, but is constant in a wide frequency range. Sadato *et al.* (1996) even found a decrease in rCBF in non-primary motor areas when a motor task was performed with increased frequency.

It has been shown that the cytoarchitectonic organization and the connections of the two parts of the supplementary motor area are different (Luppino *et al.*, 1993). The dorsal part, where activation was apparently not impaired in the patients, represents the classical somatotopically organized supplementary motor area more related to motor execution than to motor preparation (Luppino *et al.*, 1993). The rostral area of the supplementary motor area receives higher order information from the prefrontal cortex and supposedly has a role in motor control more related to movement preparation than to movement execution (Luppino *et al.*, 1993; Damasio *et al.*, 1996). The adjacent areas of the cingulate BA 32 and

Table 4

Area	Talairach coordinates			*Z*-score (significance level)	% Change in normalized rCBF	
	x	*y*	*z*		Controls	HD
(**A**) Areas with significantly greater rCBF increases in the controls than in the Huntington's disease patients						
Left striatum	30	–1	4	3.4 ($P = 0.005$)	6.2	2.9
SMA rostral/anterior cingulate (BA 6/24/32)	–3	8	40	3.1 ($P = 0.007$)	6.1	1.1
Left premotor cortex (BA 6)	46	5	52	3.1 ($P = 0.007$)	2.8	1.6
Left premotor cortex (BA 6)	24	–13	56	2.9 ($P = 0.01$)	2.5	1.5
Right premotor cortex (BA 6)	–35	5	58	4.5 ($P = 0.0005$)	3.5	1.8
Right sensorimotor cortex (BA 4)	–46	–15	52	2.9 ($P = 0.01$)	2.9	1.2
(**B**) Areas with significantly greater rCBF increases in the Huntington's disease patients than in the controls						
Left inferior parietal cortex (BA 40)	28	–46	40	3.5 ($P = 0.003$)	3.4	4.9
Right premotor cortex (BA 6)	–60	3	9	3.3 ($P = 0.005$)	0.2	4.2
Right superior parietal cortex (BA 7)	–19	–42	52	3.6 ($P = 0.003$)	0.2	5.3
Right inferior parietal cortex (BA 40)	–35	–44	40	5.1 ($P = 0.0002$)	0.5	4.4
Posterior cingulate (BA 31)	12	–15	45	3.1 ($P = 0.008$)	0.1	3.2

Brain areas showing significantly greater increases in rCBF in the control group (**A**) and in the Huntington's disease patients (HD) of Group 1 (**B**). The Talairach coordinates of the voxel in each area showing maximum significant difference in motor activation and the percentage increase in normalized rCBF for this voxel are listed.

Table 5 *Correlation analysis*

Area	Talairach coordinates			Regression coefficient	*Z*-score (significance level)
	x	*y*	*z*		
SMA/anterior cingulate (BA 6/42/32)	–4	3	40	–0.92	3.35 ($P = 0.002$)
SMA rostral/anterior cingulate (BA 6/24/32)	–12	5	38	–0.92	3.35 ($P = 0.002$)
Left parietal cortex (BA 2/40)	39	–33	54	–0.94	3.80 ($P = 0.0003$)

Talairach coordinates of the voxel in each area showing maximum significant correlation with the failure rate in all 13 patients included in the study. The table lists areas with significant negative correlation, corresponding to a decrease of rCBF response with decrease of performance. SMA = supplementary motor area.

24 are functionally closely related to the rostral supplementary motor area (Wiesendanger and Wise, 1992). Consistent with this are results obtained in PET studies in normal volunteers by Boecker *et al.* (1996), which have shown that the rostral supplementary motor area is the predominant region where activation is related to the central control of complex sequential motor tasks. Although it can be assumed that the task was more complicated for the patients than for the controls, there was no increased activation in the patients in areas attributable to the supplementary motor area or to the premotor cortex (with the exception of a small area in the inferior part of the right premotor cortex), but instead extensive hypoactivity of these non primary motor areas was present. Furthermore, these areas (rostral supplementary motor area/anterior cingulate) were those where the correlation analysis revealed an increase of activation depending on the ability to perform the given motor task. The localization of the areas appearing in this correlation analysis is similar to the region where Boecker *et al.* (1996) demonstrated in normal volunteers a dependence of activation on the complexity of a motor task. They concluded that these areas are responsible for the central on-line control of complex sequential limb movements. Their results agree with primate studies showing that lesions in these areas produce deficits in performing complex sequential movements (Wiesendanger and Wise, 1992). These findings may explain why Huntington's disease patients not able to recruit these areas cannot perform a sequential motor task adequately.

The most pronounced impairment of activation in the Huntington's disease patients of the present study was observed in the lateral premotor cortex. This area has been shown to be involved in the preparation of movements similar to the supplementary motor area and pre-supplementary motor area, but it receives striatal input from areas anatomically and functionally different from these (Hoover and Strick, 1993; Thaler *et al.*, 1995). Although there is some apparent overlap in the functional specialization, lateral premotor cortex seems to be more involved in the planning of motor action guided by external cues (Halsband and Passingham, 1985). This is reflected by the extended bilateral activation of these areas in our control population during the externally triggered motor paradigm. Differences between the activation pattern of medial and lateral premotor areas have been observed in patients with Parkinson's disease (Samuel *et al.*, 1996). In this study, equivalent impairment of activation during a sequential finger movement task to that of our Huntington's

disease patients of pre-supplementary motor area along with anterior cingulate was reported. However, in contrast to the observations in our Huntington's disease patients, the patients with Parkinson's disease in the study by Samuel *et al.* (1996) showed increased and not impaired activation of lateral premotor areas (Samuel *et al.*, 1996).

Patients with idiopathic dystonia show hyperactivation of both lateral premotor areas and the rostral supplementary motor area with the anterior cingulate during the performance of a motor task (Ceballos-Baumann *et al.*, 1995). They are similar in this respect to patients with striatocapsular infarction, where a sequential finger opposition task reveals enhanced activation in areas attributable to the supplementary motor area and lateral premotor cortex (Weiller *et al.*, 1992) with Parkinson's disease and dystonia (Playford *et al.*, 1992; Weiller *et al.*, 1992; Ceballos-Baumann *et al.*, 1995).

In addition to the parietal hyperactivity, there were small areas of the posterior cingulate and the inferior premotor cortex that showed hyperactivation in the Huntington's disease patients. This could suggest that the recruitment of additional motor related areas is necessary for Huntington's disease patients to perform this sequential motor task.

Enhanced activation in patients with Huntington's disease

Areas with enhanced activation in the patients were predominantly located in the posterior part of the brain and included the parietal cortex and the posterior cingulate. The patients showed a predominantly right-sided enhancement of activation of parietal areas covering BA 7 and 40. Correlation analysis revealed that patients with a higher activation in the left parietal cortex had better performance. Enhanced parietal activation was also observed in patients with Parkinson's disease (Samuel *et al.*, 1996). In contrast to the findings in patients with idiopathic dystonia, impaired activation of the parietal cortex (BA 5 and 7) was reported (Ceballos-Baumann *et al.*, 1995).

The parietal cortex is known to be involved in the spatial processing requirements of a given motor task. Colby and Duhamel (1991) demonstrated the selective dependence of subgroups of parietal neurons located in BA 5 and 7 on different components of motion perception necessary for hand and mouth coordination, i.e. there are neurons responding selectively to rotation of the upper limb joint. They postulate a special role of the parietal cortex in the sensory motor integration. This would implicate, for the present study, an increased demand in Huntington's disease patients for this kind of integration.

Consistent with this hypothesis are observations with PET and functional MRI, which show increasing activity of these parietal regions matching the increasing complexity of sequential finger movements or selection of one of a number of possible responses in normal subjects (Deiber *et al.*, 1991; Boecker *et al.*, 1996; Rosen *et al.*, 1996). These studies showed, in addition, an increase in activity in the secondary motor regions, the rostral supplementary motor area and lateral premotor cortex, all of which showed impaired activation in our Huntington's disease patients.

For methodological reasons, the comparison of cerebellar activation has been limited in the present study. Cerebellar hyperactivation following motor activation was reported in patients with striatocapsular infarction, but not in patients

Reorganization of the motor cortex in patients with Huntington's disease

At first sight, it is surprising that the differences in activation between Huntington's disease patients and the control population were more similar to the differences observed in patients with Parkinson's disease than in patients with the purely hyperkinetic disorder of idiopathic dystonia (Playford *et al.*, 1992; Ceballos-Baumann *et al.*, 1995; Samuel *et al.*, 1996).

However, as already mentioned, the pattern of activation impairment was not completely equivalent in Parkinson's disease and Huntington's disease patients. Activation of lateral prefrontal areas was impaired in Huntington's disease patients but enhanced in Parkinson's disease patients (Samuel *et al.*, 1996). Although the motor task in the present study was not directly comparable with that used in the study of Ceballos-Baumann *et al.* (1995) on patients with idiopathic dystonia, it revealed a similar pattern of enhanced and impaired activation of frontal and parietal areas in Huntington's disease.

If one assumes a critical role of the direct and the indirect pathway of the basal ganglia-thalamo-cortical motor circuit in the activation of the above-mentioned non-primary frontal motor areas, the differences and similarities of the activation patterns are easily explained (DeLong, 1990).

In Huntington's disease, there is the apparent paradox of the coexistence of chorea and bradykinesia. Thompson *et al.* (1988) attributed this to both pathways, the direct and the indirect pathway of the basal ganglia-thalamo-cortical motor circuit being underactive in Huntington's disease. This assumption is consistent with the results in the present study, which have demonstrated the hypoactivity in this disease of all areas in the mesial and lateral frontal cortex representing the frontal lobe targets that receive basal ganglia output of the motor portion of the basal ganglia-thalamo-cortical circuits.

It has been proposed that the involuntary movements exhibited in idiopathic dystonia are a result not of underactivity, but of overactivity of both pathways (Hallet, 1993). Assuming this, one would expect hyperactivation in the frontal lobe targets of the motor portion of the basal ganglia-thalamo-cortical circuits, a situation mirrored to Huntington's disease. This was indeed observed by Ceballos-Baumann *et al.* (1995). Akinetic–rigid Parkinson's disease is thought to be associated with reduced direct and increased indirect pathway activity (Hallet, 1993). The observed pattern

of enhanced and impaired activation in functionally different frontal non-primary motor areas would be consistent with this (Playford *et al*. 1992).

So it is tempting to speculate that in Huntington's disease the lack of basal ganglia input via both pathways, to the thalamus and hence into the premotor target areas, is the prime cause of the impaired activation during sequential finger movements, rather than the lack of prefrontal input into these areas, although prefrontal atrophy is reported in patients in more advanced stages of disease (Kuwert *et al.*, 1993).

Consistent with this view is the observation that Huntington's disease patients are able to recruit motor-related parietal areas in an equivalent way to Parkinson's disease patients (Playford *et al.*, 1992; Samuel *et al.*, 1996). Activation of these areas is not critically dependent on basal ganglion input (Colby and Duhamel, 1991). The hypothesis raised in studies with Parkinson's disease patients that impaired basal ganglion function induces a shift from the frontal motor circuit, which includes the basal ganglia, towards a loop supporting motor action, including the parietal cortex, is supported by the observations in the present study (Playford *et al.*, 1992; Samuel *et al.*, 1996).

The dependence of the ability to coordinate sequential externally triggered movements with the ability to activate the rostral cingulate and supplementary motor area for Huntington's disease patients was demonstrated in the correlation analysis. These areas are equivalent to those shown to be hypoactive in Parkinson's disease (Samuel *et al.*, 1996). This may indicate that, although rigidity and akinesia in Huntington's disease patients in the early stages of disease are not dominant, impairment of the direct pathway could have affected more the ability to perform the automated motor task correctly. This finding can be explained partly by the design of the study. All patients exhibiting relevant choreatic hyperkinesias during the scan were excluded. Thus any hyperkinetic component was minimized in the Huntington's disease patients that were analysed, which would directly influence the measured motor action. The aim of controlling involuntary movements as much as possible has led to selection bias towards patients with more hypokinetic forms of Huntington's disease, although bradykinesia and rigidity were not predominant in these patients. But the fact that rostral cingulate and supplementary motor area are the main areas appearing in the correlation analysis is also a strong indicator of their critical importance for the coordinated execution of an externally triggered motor task (Damasio *et al.*, 1996). The degree to which Huntington's disease patients are able to recruit these areas, rather than the total impairment of basal ganglion function itself, may determine their ability to perform automated motor tasks adequately.

Conclusion

This study has demonstrated, in patients with Huntington's disease, impaired activity of the striatum and its frontal motor projection areas and enhanced activity mainly of parietal motor related areas, during voluntary movement. This imbalance in cerebral function can be explained in terms of the pathology of Huntington's disease, which leads to global impairment of all output channels of the basal ganglia-thalamo-cortical motor circuit projecting to the cortex and the compensatory recruitment of additional accessory motor pathways involving the parietal cortex.

Acknowledgements

We wish to thank our radiochemistry group and the cyclotron staff for their reliable supply of the radiopharmaceuticals; Ms C. Kruschke and Mr H. Riescher for their technical assistance; Mrs J. Neverve and Ms N. Nguyen for careful review of the manuscript; Dr K. Friston and Professor R. S. J. Frackowiack, Wellcome Department of Cognitive Neurology, Institute of Neurology, London for generously providing us with the SPM software to process our results; Professor C. Weiller and Dr S. Kiebel, Department of Neurology, University of Jena for help during the installation and evaluation of this program. We also wish to thank the members of the Deutsche Huntington-Selbsthilfegruppe for their willingness to participate in this study. The study was supported by the Deutsche Forschungsgemeinschaft (SFB 462, Sensomotorik).

References

Alexander GE, Crutcher MR, DeLong MR. Basal ganglia-thalamocortical circuits: parallel substrates for motor, oculomotor, 'prefrontal' and 'limbic' functions. [Review]. Progr Brain Res 1990; 85: 119–46.

Blinkenberg M, Bonde C, Holm S, Svarer C, Andersen J, Paulson OB, et al. Rate dependence of regional cerebral activation during performance of a repetitive motor task: a PET study. J Cereb Blood Flow Metab 1996; 16: 794–803.

Boecker H, Ceballos-Baumann A, Dagher A, Samuel M, Passingham RE, Friston KJ, et al. Central processing of increasingly complex learned finger sequences: correlational analysis of 3D $H_2^{15}O$ PET data [abstract]. Neurology 1996; 46 (2 Suppl): A382.

Ceballos-Baumann AO, Passingham RE, Warner T, Playford ED, Marsden CD, Brooks DJ. Overactive prefrontal and underactive motor cortical areas in idiopathic dystonia. Ann Neurol 1995; 37: 363–72.

Colby CL, Duhamel JLR. Heterogeneity of extrastriate visual areas and multiple parietal areas in the macaque monkey. [Review]. Neuropsychologia 1991; 29: 517–37.

Colebatch JG, Deiber MP, Passingham RE, Friston KJ, Frackowiak RS. Regional cerebral blood flow during voluntary arm and hand movements in human subjects. J Neurophysiol 1991; 65: 1392–401.

Damasio AR, Damasio H, Christen Y. Neurobiology of decision-making. Heidelberg: Springer, 1996.

Deiber M-P, Passingham RE, Colebatch JG, Friston KJ, Nixon PD, Frackowiak RSJ. Cortical areas and the selection of movement: a

study with positron emission tomography. Exp Brain Res 1991; 84: 393–402.

DeLong MR. Primate models of movement disorders of basal ganglia origin. Trends Neurosci 1990; 13: 281–5.

Duyao M, Ambrose C, Myers R, Noveletto A, Persichetti F, Frontali M, et al. Trinucleotide repeat length instability and age of onset in Huntington's disease [see comments]. Nat Genet 1993; 4: 387–92. Comment in: Nat Genet 1993; 4: 329–30.

Fox PT, Raichle ME. Stimulus rate dependence of regional cerebral blood flow in human striate cortex, demonstrated by positron emission tomography. J Neurophysiol 1984; 51: 1109–20.

Fox PT, Fox JM, Raichle ME, Burde RM. The role of cerebral cortex in the generation of voluntary saccades: a positron emission tomographic study. J Neurophysiol 1985; 54: 348–69.

Friston KJ, Frith CD, Liddle PF, Frackowiak RS. Comparing functional (PET) images: the assessment of significant change. J Cereb Blood Flow Metab 199; 11: 690–9.

Girotti F, Carella F, Scigliano G, Grassi MP, Soliveri P, Giovannini P, et al. Effect of neuroleptic treatment on involuntary movements and motor performances in Huntington's disease. J Neurol Neurosurg Psychiatry 1984; 47: 848–52.

Grafton ST, Mazziotta JC, Pahl JJ, St. George-Hyslop P, Haines JL, Gusella J, et al. Serial changes of cerebral glucose metabolism and caudate size in persons at risk for Huntington's disease. Arch Neurol 1992; 49: 1161–7.

Hallett M, Ravits J. Involuntary Movements. In: Asbury AK, McKhann GM, McDonald WI, editors. Diseases of the nervous system. Clinical Neurobiology. Philadelphia: W.B. Saunders, 1986: 452–60.

Hallett M. Physiology of basal ganglia disorders: an overview. [Review]. Can J Neurol Sci 1993; 20: 177–83.

Halsband U, Passingham RE. Premotor cortex and the conditions for movement in monkeys (Macaca fascicularis). Behav Brain Res 1985; 18: 269–77.

Hoover JE, Strick PL. Multiple output channels in the basal ganglia. Science 1993; 259: 819–21.

Huntington's Disease Collaborative Research Group. A novel gene containing a trinucleotide repeat that is expanded and unstable on Huntington's disease chromosomes [see comments]. Cell 1993; 72: 971–983. Comment in: Cell 1993; 72: 817–8.

Kanazawa I, Tanaka Y, Cho F. 'Choreic' movements induced by unilateral kainate lesion of the striatum and L-DOPA administration in monkey. Neurosci Lett 1986; 71: 241–6.

Kew JJ, Goldstein LH, Leigh PN, Abrahams S, Cosgrave N, Passingham RE, et al. The relationship between abnormalities of cognitive function and cerebral activation in amyotrophic lateral sclerosis. A neuropsychological and positron emission tomography study. Brain 1993; 116: 1399–423.

Kuhl DE, Phelps ME, Markham CH, Metter EJ, Riege WH, Winter J. Cerebral metabolism and atrophy in Huntington′s disease determined by 18FDG and computed tomographic scan. Ann Neurol 1982; 12: 425–34.

Kuwert T, Lange HW, Boecker H, Titz H, Herzog H, Aulich A, et al. Striatal glucose consumption in chorea-free subjects at risk of Huntington's disease [see comments]. J Neurol 1993; 241: 31–6. Comment in: J Neurol 1995; 242: 112–4.

Lane RD, Glazer WM, Hansen TE, Berman WH, Kramer SI. Assessment of tardive dyskinesia: using the Abnormal Involuntary Movement Scale. J Nerv Ment Dis 1985; 173: 353–7.

Lange H, Thörner G, Hopf A, Schröder KF. Morphometric studies of the neuropathological changes in choreatic diseases. J Neurol Sci 1976; 28: 401–25.

Leenders KL, Frackowiak RSJ, Quinn N, Marsden CD. Brain energy metabolism and dopaminergic function in Huntington's disease measured in vivo using positron emission tomography. Mov Disord 1986; 1: 69–77.

Luppino G, Matelli M, Camarda R, Rizzolatti G. Corticocortical connections of area F3 (SMA-proper) and area F6 (pre-SMA) in the macaque monkey. J Comp Neurol 1993; 338: 114–40.

Martin JB. Molecular genetics of neurological diseases [published erratum appears in Science 1994; 264: 644]. [Review]. Science 1993; 262: 674–6.

Mayeux R, Stern Y, Herman A, Greenbaum L, Fahn S. Correlates of early disability in Huntington's disease. Ann Neurol 1986; 20: 727–31.

Minoshima S, Koeppe RA, Mintun MA, Berger KL, Taylor SF, Frey KA, et al. Automated detection of the intercommissural line for stereotactic localization of functional brain images. J Nucl Med 1993; 34: 322–9.

Minoshima S, Koeppe RA, Frey KA, Kuhl DE. Anatomic standardization: linear scaling and nonlinear warping of functional brain images. J Nucl Med 1994; 35: 1528–37.

Minoshima S, Frey KA, Koeppe RA, Foster NL, Kuhl DE. A diagnostic approach in Alzheimer's disease using three-dimensional stereotactic surface projections of [F-18]FDG PET. J Nucl Med 1995; 36: 1238–48.

Myers RH, Vonsattel JP, Stevens TJ, Cupples LA, Richardson EP, Martin JB, et al. Clinical and neuropathologic assessment of severity in Huntington's disease. Neurology 1988; 38: 341–7.

Myers RH, Vonsattel JP, Paskevich PA, Kiely DK, Stevens TJ, Cupples LA, et al. Decreased neuronal and increased oligodendroglial densities in Huntington's disease caudate nucleus. J Neuropathol Exp Neurol 1991; 50: 729–42.

Oldfield RC. The assessment and analysis of handedness: Edinburgh inventory. Neuropsychologia 1971; 9: 97–113.

Playford ED, Jenkins IH, Passingham RE, Nutt J, Frackowiak RS, Brooks DJ. Impaired mesial frontal and putamen activation in Parkinson's disease: a positron emission tomography study. Ann Neurol 1992; 32: 151–61.

Rosen AC, Rao SM, Haaland KY, Harrington DL, Bobholz JA, Woodley SJ, et al. Brain systems for generating heterogeneous finger movement sequences. Neuroimage 1996; 3: S369.

Roth EM, Tym E, Mountjoy CQ, Huppert FA, Hendrie H, Verma S, et al. CAMDEX. A standardised instrument for the diagnosis of mental disorder in the elderly with special reference to the early detection of dementia. Br J Psychiatry 1986; 149: 698–709.

Sadato N, Ibanez V, Deiber M-P, Campbell G, Leonardo M, Hallet M. Frequency-dependent changes of regional cerebral blood flow during finger movements. J Cereb Blood Flow Metab 1996; 16: 23–33.

Samuel M, Ceballos-Baumann A, Blin J, Uema T, Boecker H, Krams M, et al. Unimanual and bimanual sequential finger movements in normal individuals and Parkinson's disease patients: a study using positron emission tomography [abstract]. Neurology 1996; 46 (2 Suppl): A455.

Stephan KM, Fink GR, Passingham RE, Silbersweig D, Ceballos-Baumann AO, Frith CD, et al. Functional anatomy of the mental representation of upper extremity movements in healthy subjects. J Neurophysiol 1995; 73: 373–86.

Talairach J, Tournoux P. Co-planar stereotaxic atlas of the human brain. Stuttgart: Thieme, 1988.

Thaler D, Chen Y-C, Nixon PD, Stern CE, Passingham RE. The functions of the medial premotor cortex: I. Simple learned movements. Exp Brain Res 1995; 102: 445–60.

Thompson PD, Berardelli A, Rothwell JC, Day BL, Dick JP. The coexistence of bradykinesia and chorea in Huntington's disease and its implications for theories of basal ganglia control of movement. Brain 1988; 111: 223–44.

Vonsattel JP, Myers RH, Stevens TJ, Ferrante RJ, Bird ED, Richardson EP Jr. Neuropathological classification of Huntington's disease. J Neuropathol Exp Neurol 1985; 44: 559–77.

Weiller C, Chollet F, Friston KJ, Wise RSJ, Frackowiak RSJ. Functional reorganization of the brain in recovery from striatocapsular infarction in man. Ann Neurol 1992; 31: 463–72.

Wenzel R, Bartenstein P, Dieterich M, Danek A, Weindl A, Minoshima S, et al. Deactivation of human visual cortex during involuntary ocular oscillations: a PET activation study . Brain 1996; 119: 101–10.

Wiesendanger M, Wise SP. Current issues concerning the functional organization of motor cortical areas in nonhuman primates. [Review]. Adv Neurol 1992; 57: 117–34.

Worsley KJ, Evans AC, Marrett S, Neelin P. A three-dimensional statistical analysis for CBF activation studies in human brain [see comments]. J Cereb Blood Flow Metab 1992; 12: 900–18. Comment in: J Cereb Blood Flow Metab 1993; 13: 1040–2.

Received April 1, 1997. Accepted May 3, 1997